Electronic Supplementary Material (ESI) for Physical Chemistry Chemical Physics.

Supporting Information

Nucleophilic Substitution Reactions of Microsolvated Hydroperoxide Anion $HOO^-(NH_3)_n$ with Methyl Chloride and Comparison Between Ammonia and Water as Solvent

Yang Hu, Xiangyu Wu, Jing Xie*

Key Laboratory of Cluster Science of Ministry of Education, Beijing Key Laboratory of Photoelectronic/Electrophotonic Conversion Materials, School of Chemistry and Chemical Engineering, Beijing Institute of Technology, Beijing 100081, China

Table of Contents

Figures

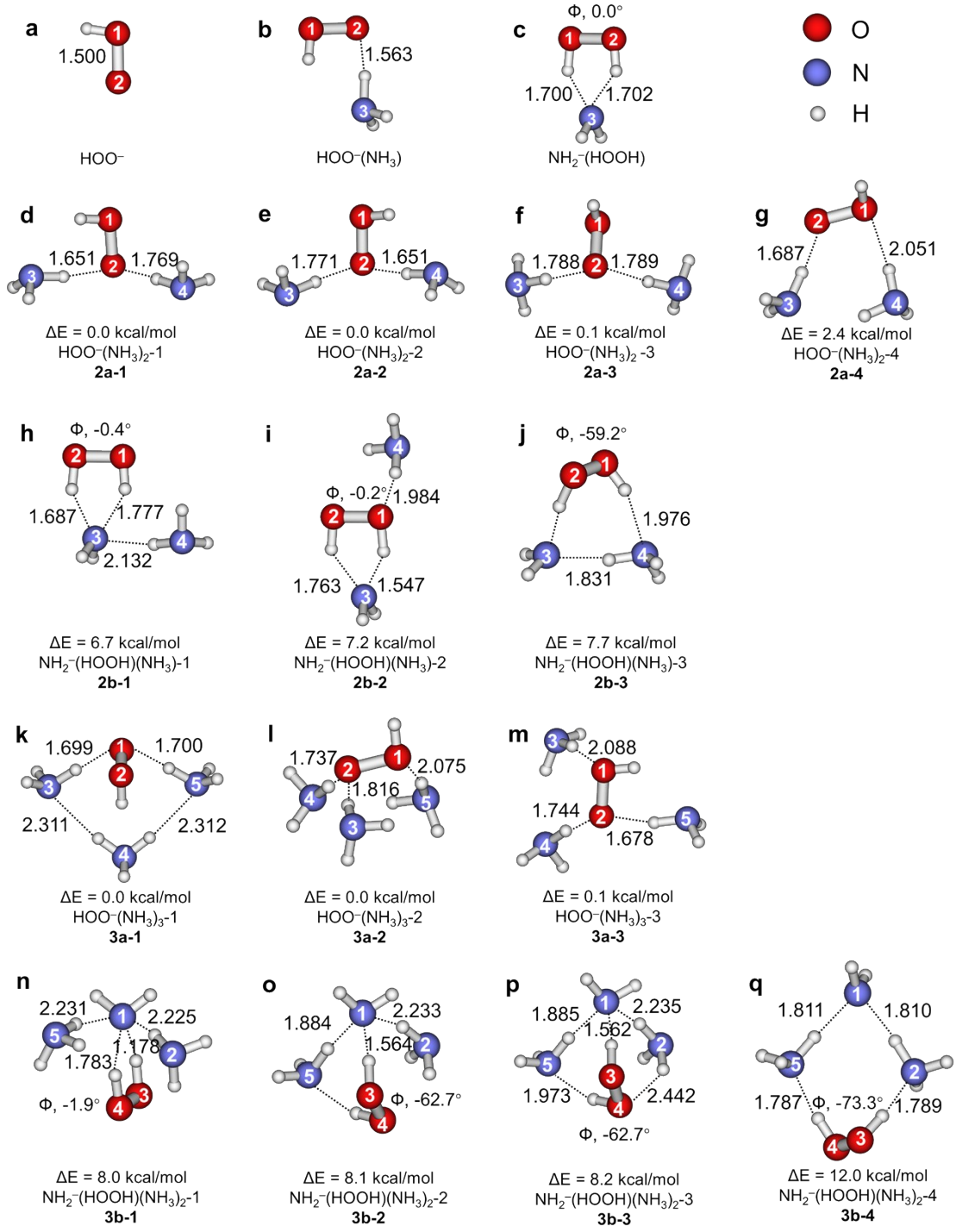

Figure S1. Structures of $HOO^{-}(NH_3)_{n=0-3}$ isomers as optimized with MP2/6-311++G(d,p) method. Relative energies ΔE (in kcal/mol) computed with CCSD(T)/aug-cc-pVTZ//MP2/6-311++G(d,p) method are shown for isomers of $HOO^{-}(NH_3)_2$.

Potential Energy Profiles (PESs)

Note: For following PESs, the relative electronic energy (in kcal/mol) and enthalpy values at 298.15 K that computed at CCSD(T) level of theory are present. Color code: H, white; C, blue; N, purple; O, red; Cl, green.

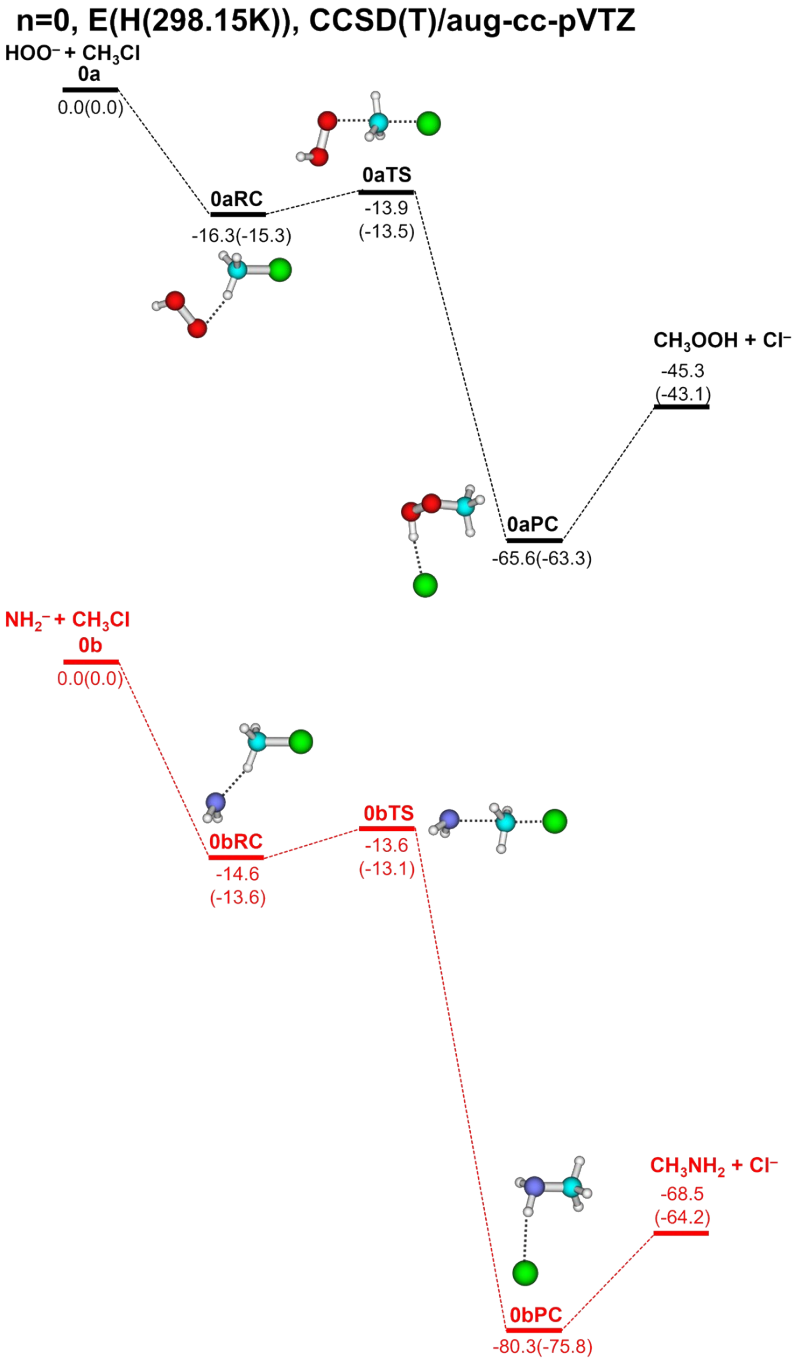

Figure S2. Potential energy profile of (top) $HOO^- + CH_3Cl \rightarrow CH_3OOH + Cl^-$ reaction and (bottom) $NH_2^- + CH_3Cl \rightarrow CH_3NH_2 + Cl^-$ reaction.

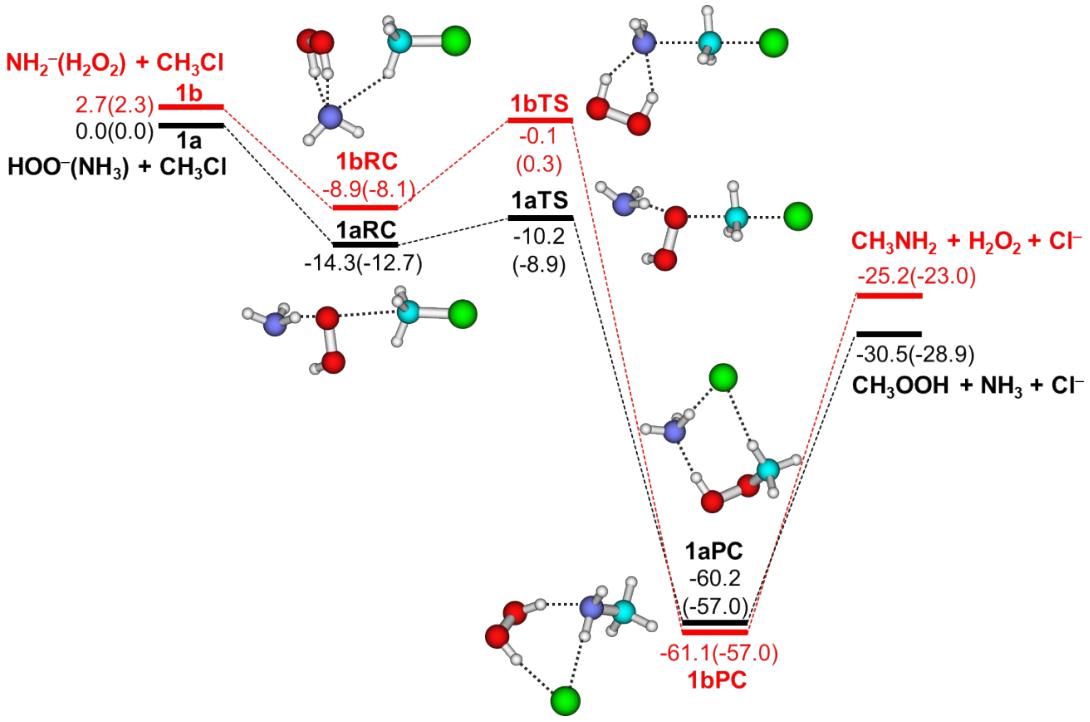

Figure S3. Potential energy profile of $HOO^{-}(NH_3) + CH_3Cl \rightarrow CH_3OOH + NH_3 + Cl^{-}$ and $NH_2^{-}(HOOH) + CH_3Cl \rightarrow CH_3NH_2 + HOOH + Cl^{-}$ reaction.

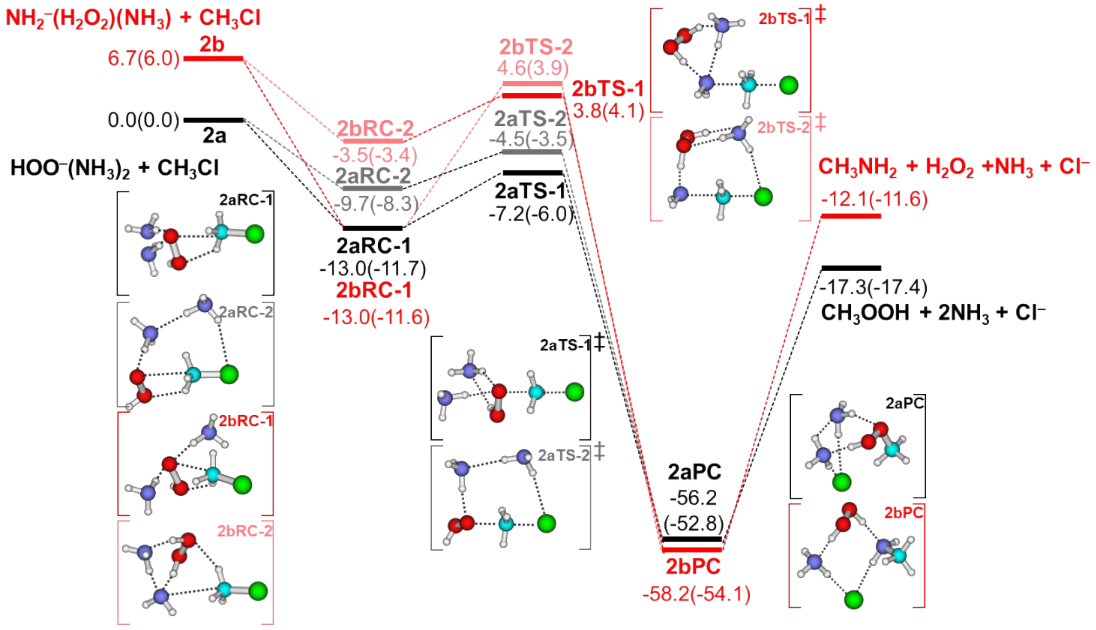

Figure S4. Potential energy profile of $HOO^{-}(NH_3)_2 + CH_3Cl \rightarrow CH_3OOH + 2NH_3 + Cl^{-}$ and $NH_2^{-}(HOOH)(NH_3) + CH_3Cl \rightarrow CH_3NH_2 + HOOH + NH_3 + Cl^{-}$ reaction.

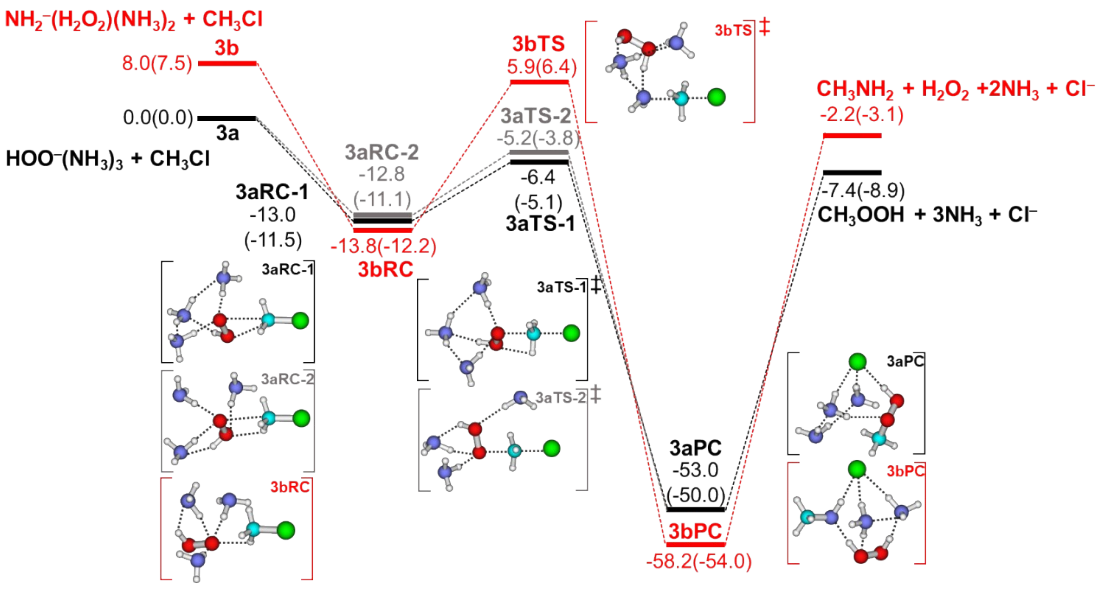

Figure S5. Potential energy profile of $HOO^{-}(NH_3)_3 + CH_3Cl \rightarrow CH_3OOH + 3NH_3 + Cl^{-}$ and $NH_2^{-}(HOOH)(NH_3)_2 + CH_3Cl \rightarrow CH_3NH_2 + HOOH + 2NH_3 + Cl^{-}$ reaction.

n=0

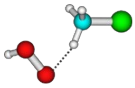

0aRC-1

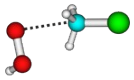

0aRC-2

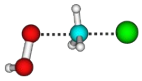

0aTS-1

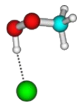

0aPC-1

n=1

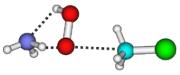

1aRC-1

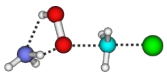

1aTS-1

1aPC-1

1aPC-2

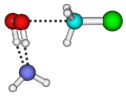

1bRC-1

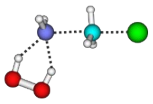

1bTS-1

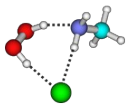

1bPC-1

n=2

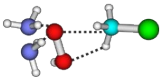

2aRC-1

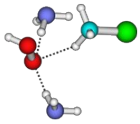

2aRC-2

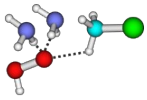

2aRC-3

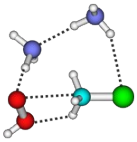

2aRC-4

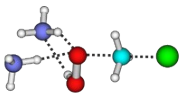

2aTS-1

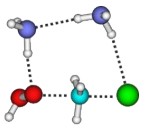

2aTS-2

2aPC-1

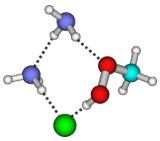

2aPC-2

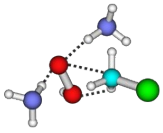

2bRC-1

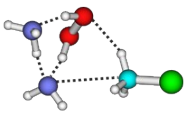

2bRC-2

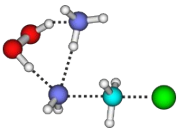

2bTS-1

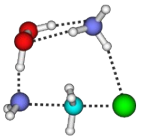

2bTS-2

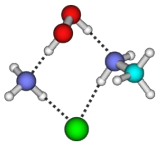

2bPC-1

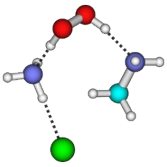

2bPC-2

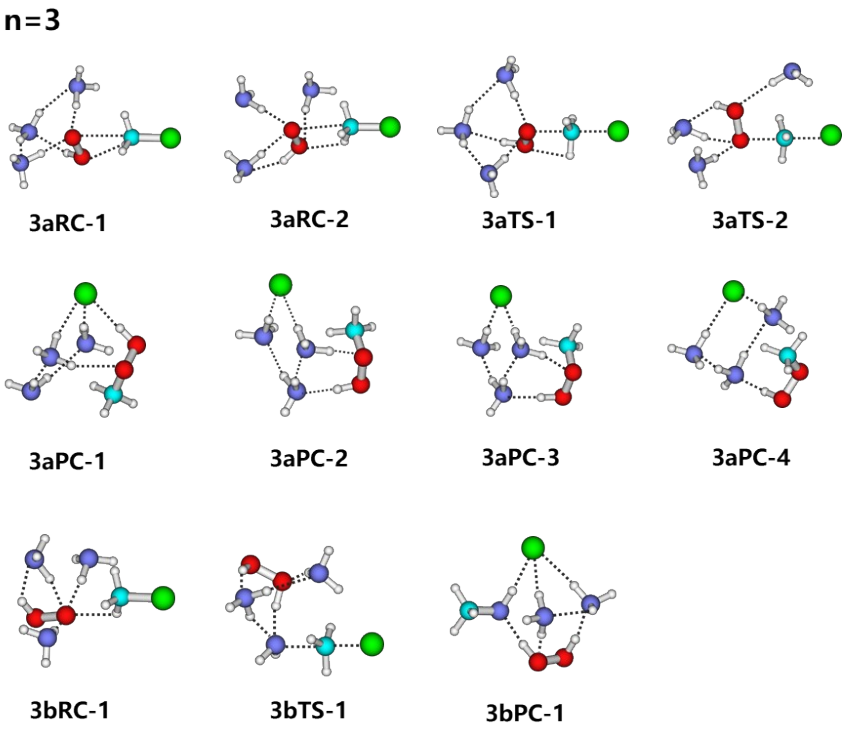

Figure S6. Structures of the stationary points for $HOO^{-}(NH_3)_{n=0-3}$ + CH_3Cl reactions optimized at MP2/6-311++G(d,p) level of theory. Color code: H, white; C, blue; N, purple; O, red; Cl, green.

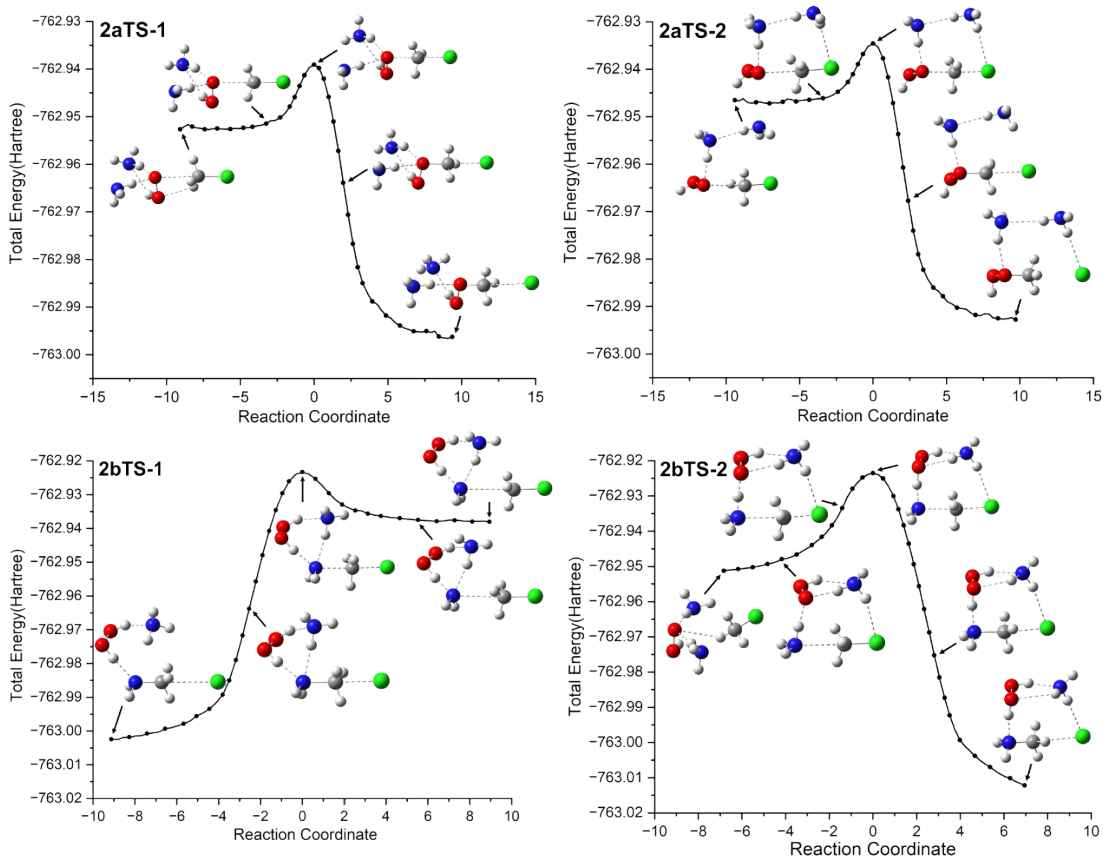

Figure S7. Intrinsic reaction coordinates (IRC) calculation of 2aTS-1, 2aTS-2, 2bTS-1, 2bTS-2 transition states of $HOO^{-}(NH_3)_2$ + CH_3Cl reactions using MP2/6-311++G(d,p) method. Color code: H, white; C, blue; N, purple; O, red; Cl, green.

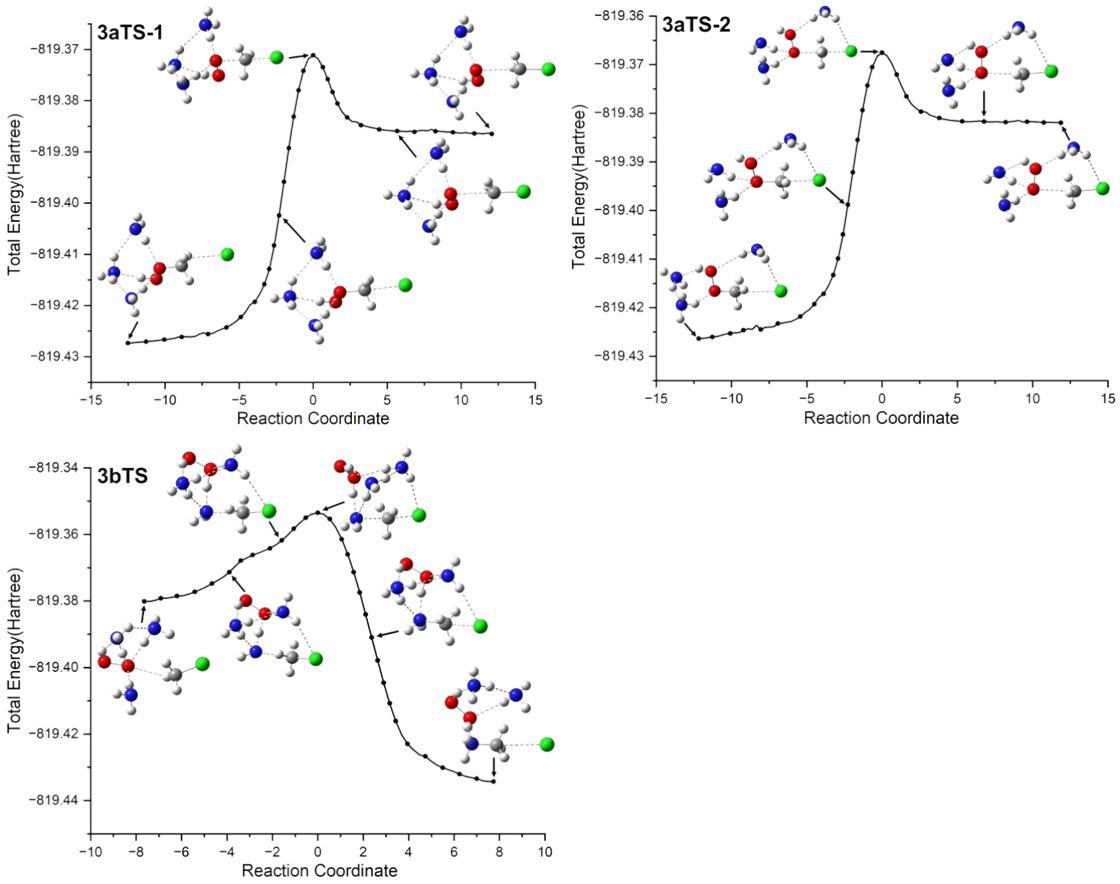

Figure S8. Intrinsic reaction coordinates (IRC) calculation of 3aTS-1, 3aTS-2 and 3bTS transition states of $HOO^{-}(NH_3)_3$ + CH_3Cl reactions using MP2/6-311++G(d,p) method. Color code: H, white; C, blue; N, purple; O, red; Cl, green.

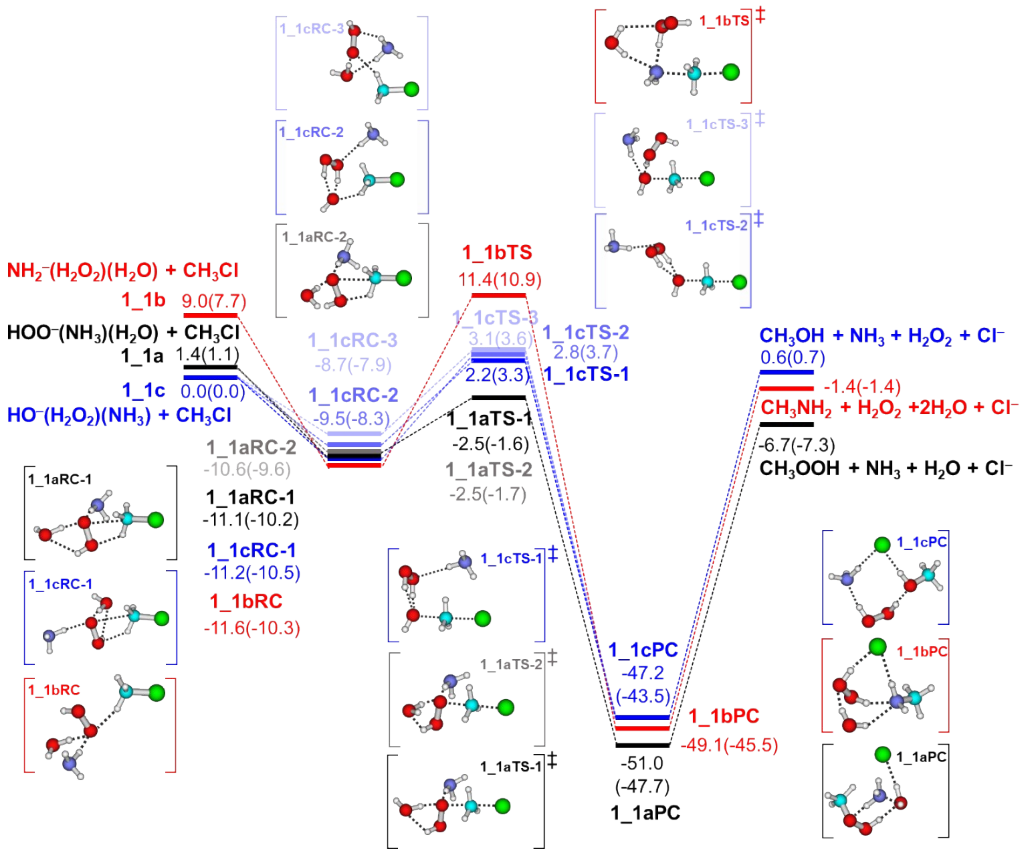

Figure S9. Potential energy profile of $HOO^{-}(NH_3)(H_2O) + CH_3Cl \rightarrow CH_3OOH + NH_3 + H_2O + Cl^{-}$ and $NH_2^{-}(HOOH)(H_2O) + CH_3Cl \rightarrow CH_3NH_2 + HOOH + NH_3 + Cl^{-}$, and $HO^{-}(HOOH)(NH_3) + CH_3Cl \rightarrow CH_3OH + HOOH + NH_3 + Cl^{-}$ reaction.

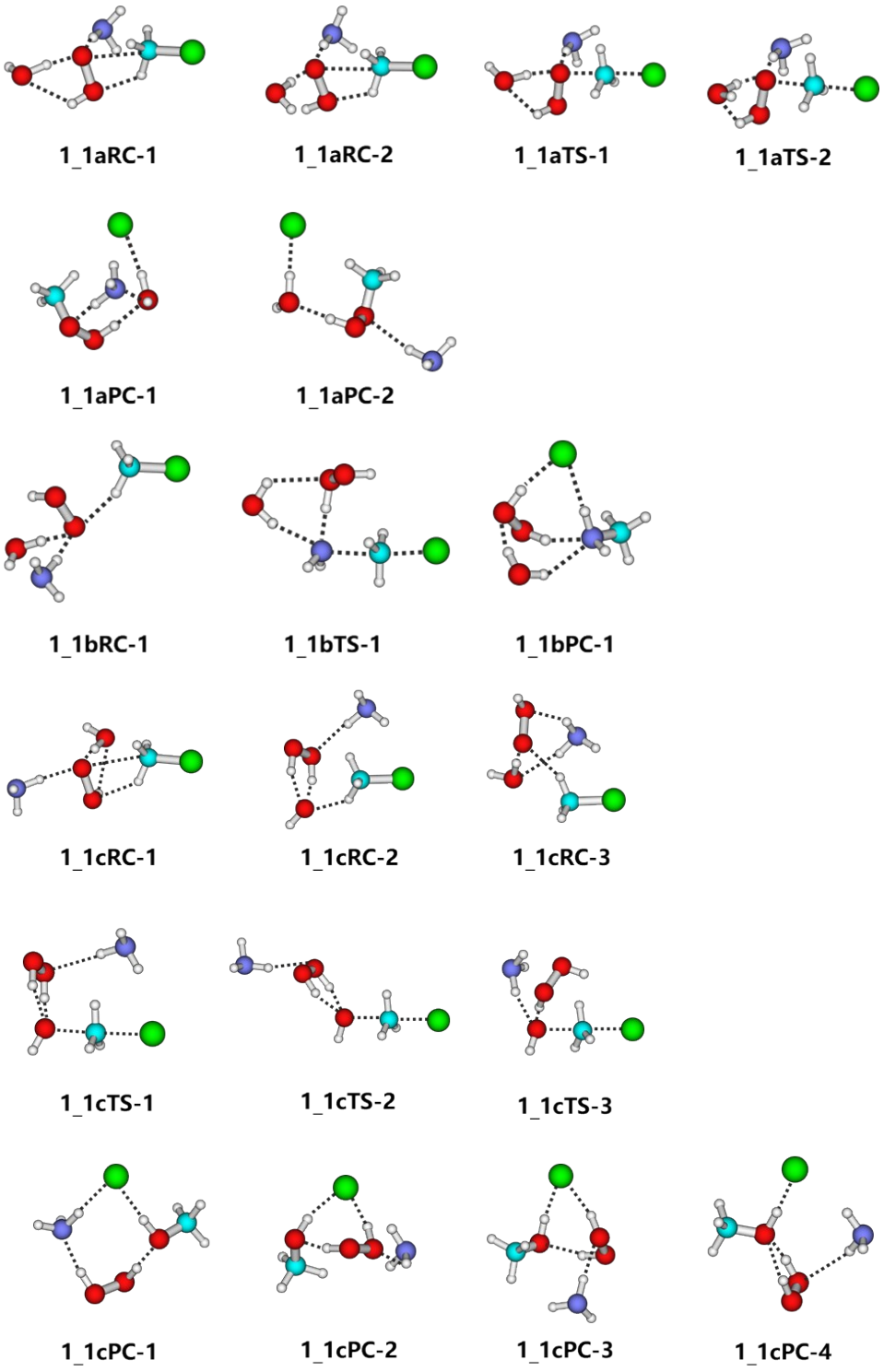

Figure S10. Structures of the stationary points for $HOO^{-}(NH_3)(H_2O)$ + CH_3Cl optimized at MP2/6-311++G(d,p) level of theory. Color code: H, white; C, blue; N, purple; O, red; Cl, green.

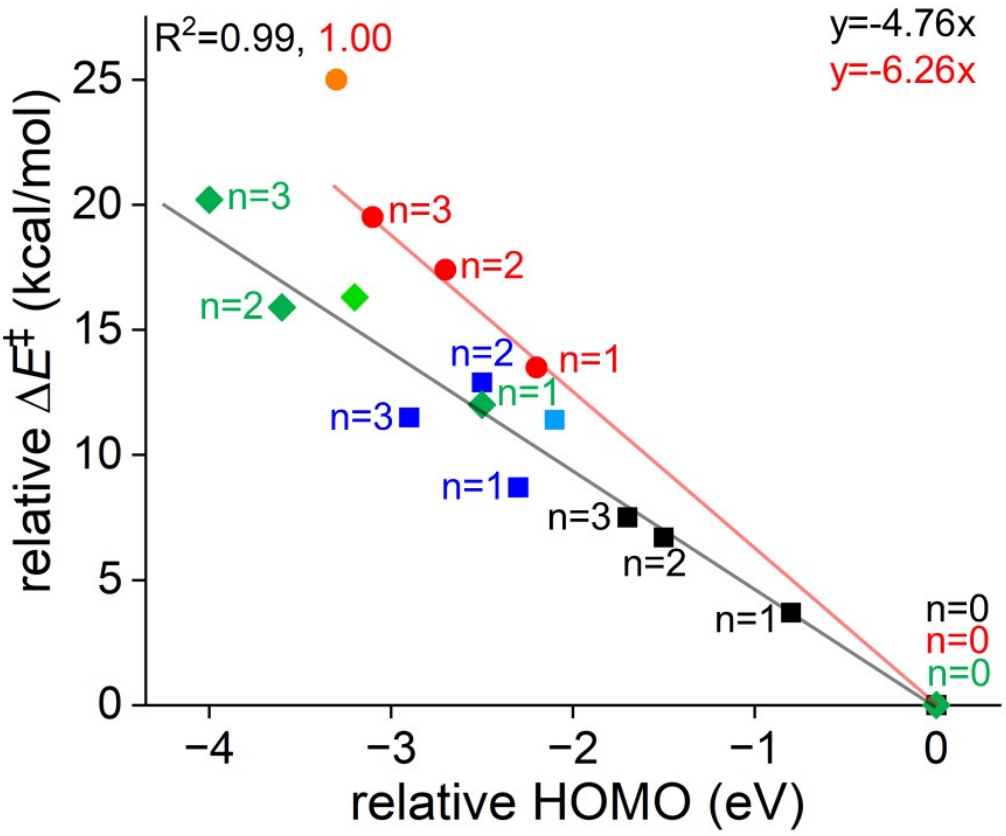

Figure S11. Correlations between relative barrier heights of $HOO^-(sol)_n$ + CH_3Cl reactions and relative HOMO level of nucleophiles. Color code: for sol = NH_3, HOO^--S_N2 path, black, NH_2^--S_N2 pathway, red; for sol = H_2O, HOO^--S_N2 path, blue, HO^--S_N2 pathway, green.

Table S1. Reaction energetics (kcal/mol) of $HOO^{-}(NH_3)$ + CH_3Cl S_N2 reactions in relative to the most stable reactants. Values are given by CCSD(T)/aug-cc-pVTZ//MP2/6-311++G(d,p) method.

Attacking Nucleophile	Products	ΔE	Δ(E+ZPE)	ΔH(298.15K)	ΔG(298.15K)	
HOO^{-} (NH_3)	$CH_3OOH + Cl^{-} + NH_3$	-30.5	-29.4	-28.9	-35.1	(1a)
	$CH_3OOH(NH_3) + Cl^{-}$	-39.3	-36.2	-35.9	-34.1	(1a′)
	$CH_3OOH + Cl^{-}(NH_3)$	-39.5	-37.5	-37.5	-38.0	(1a″)
	$(CH_3OOH)Cl^{-} + NH_3$	-50.8	-49.1	-49.1	-48.1	(1a‴)
NH_2^{-} (H_2O_2)	$CH_3NH_2 + Cl^{-} + H_2O_2$	-25.2	-23.2	-23.0	-28.9	(1b)
	$(CH_3NH_2)Cl^{-} + H_2O_2$	-37.1	-34.5	-34.6	-34.7	(1b′)
	$CH_3NH_2(H_2O_2) + Cl^{-}$	-37.2	-33.3	-33.2	-30.7	(1b″)
	$CH_3NH_2 + Cl^{-}(H_2O_2)$	-49.4	-46.8	-47.2	-46.8	(1b‴)

Table S2. Reaction energetics (kcal/mol) of $HOO^-(NH_3)_2$ + CH_3Cl S_N2 reactions in relative to the most stable reactants. Values are given by CCSD(T)/aug-cc-pVTZ//MP2/6-311++G(d,p) method.

Attacking Nucleophile	Products	ΔE	Δ(E+ZPE)	ΔH(298.15K)	ΔG(298.15K)	
$HOO^-(NH_3)_2$	$CH_3OOH + Cl^- + 2NH_3$	-17.3	-18.2	-17.4	-31.7	(2a)
	$CH_3OOH+Cl^-+(NH_3)_2$	-20.6	-20.0	-19.3	-27.8	(2a′)
	$CH_3OOH(NH_3) + Cl^- + NH_3$	-26.1	-25.0	-24.5	-30.7	(2a″)
	$CH_3OOH + Cl^-(NH_3) + NH_3$	-26.4	-26.3	-26.1	-34.6	(2a‴)
	$CH_3OOH(NH_3)_2+Cl^-$	-34.0	-30.7	-30.8	-27.0	(2a⁗)
	$CH_3OOH(NH_3) + Cl^-(NH_3)$	-35.2	-33.1	-33.2	-33.6	(2a⁗′)
	$CH_3OOH + Cl^-(NH_3)_2$	-35.6	-34.0	-34.0	-34.5	(2a⁗″)
$NH_2^-(H_2O_2)(NH_3)$	$CH_3NH_2 + Cl^- + H_2O_2 + NH_3$	-12.1	-12.0	-11.6	-25.6	(2b)
	$CH_3NH_2(NH_3)+Cl^-+HOOH$	-17.7	-16.1	-15.7	-22.5	(2b′)
	$CH_3NH_2 + Cl^- +(NH_3)(H_2O_2)$	-21.1	-18.9	-18.8	-25.2	(2b″)
	$CH_3NH_2 + Cl^-(NH_3) + H_2O_2$	-21.1	-20.1	-20.2	-28.5	(2b‴)
	$CH_3NH_2(H_2O_2)+Cl^-+NH_3$	-24.1	-22.0	-21.8	-27.3	(2b⁗)
	$CH_3NH_2(H_2O_2)(NH_3) + Cl^-$	-30.9	-27.2	-27.2	-24.0	(2b⁗′)
	$CH_3NH_2(H_2O_2) + Cl^-(NH_3)$	-33.1	-30.1	-30.5	-30.2	(2b⁗″)
	$CH_3NH_2 + Cl^-(H_2O_2) + NH_3$	-36.3	-35.6	-35.7	-43.4	(2b⁗‴)
	$CH_3NH_2(NH_3) + Cl^-(H_2O_2)$	-41.9	-39.7	-39.9	-40.4	(2b⁗⁗)
	$CH_3NH_2+Cl^-(NH_3)(H_2O_2)$	-44.6	-42.4	-42.6	-41.9	(2b⁗⁗′)

Table S3. Reaction energetics (kcal/mol) of $HOO^-(NH_3)_3$ + CH_3Cl S_N2 reactions in relative to the most stable reactants. Values are given by CCSD(T)/aug-cc-pVTZ//MP2/6-311++G(d,p) method.

Attacking Nucleophile	Products	ΔE	Δ(E+ZPE)	ΔH(298.15K)	ΔG(298.15K)	
$HOO^-(NH_3)_3$	$CH_3OOH + Cl^- + 3NH_3$	-7.4	-10.2	-8.9	-33.4	(3a)
	$CH_3OOH(NH_3) + Cl^- + 2NH_3$	-16.2	-16.9	-16.0	-32.4	(3a′)
	$CH_3OOH + Cl^-(NH_3) + 2NH_3$	-16.5	-18.3	-17.6	-36.3	(3a″)
	$CH_3OOH+Cl^-+(NH_3)_3$	-18.3	-17.0	-16.8	-24.2	(3a‴)
	$CH_3OOH(NH_3)_2 + Cl^- + NH_3$	-24.1	-22.7	-22.3	-28.8	(3a⁗)
	$CH_3OOH(NH_3) + Cl^-(NH_3) + NH_3$	-25.3	-25.0	-24.6	-35.4	(3a⁗′)
	$CH_3OOH + Cl^-(NH_3)_2 + NH_3$	-25.7	-26.0	-25.4	-36.3	(3a⁗″)
	$CH_3OOH(NH_3)_3+Cl^-$	-29.9	-27.1	-26.7	-24.8	(3a⁗‴)
	$CH_3OOH(NH_3)_2 + Cl^-(NH_3)$	-33.1	-30.8	-30.9	-31.7	(3a⁗⁗)
	$CH_3OOH(NH_3) + Cl^-(NH_3)_2$	-34.5	-32.7	-32.5	-35.3	(3a⁗⁗′)
	$CH_3OOH + Cl^-(NH_3)_3$	-36.0	-34.2	-34.1	-34.6	(3a⁗⁗″)
$NH_2^-(H_2O_2)(NH_3)_2$	$CH_3NH_2 + Cl^- + H_2O_2 + 2NH_3$	-2.2	-4.0	-3.1	-27.3	(3b)
	$CH_3NH_2(NH_3) + Cl^- + H_2O_2 + NH_3$	-7.7	-8.1	-7.2	-24.3	(3b′)
	$CH_3NH_2(H_2O_2)+Cl^-+2NH_3$	-14.1	-14.0	-13.3	-29.1	(3b″)
	$CH_3NH_2(NH_3)_2+Cl^-+H_2O_2$	-15.1	-13.4	-13.0	-20.5	(3b‴)
	$CH_3NH_2 + Cl^- + (NH_3)_2(H_2O_2)$	-18.9	-16.5	-16.5	-23.7	(3b⁗)
	$CH_3NH_2 + Cl^-(NH_3)_2 + H_2O_2$	-20.5	-19.8	-19.6	-30.2	(3b⁗′)
	$CH_3NH_2 + Cl^-(H_2O_2) + 2NH_3$	-26.4	-27.5	-27.2	-45.2	(3b⁗″)
	$CH_3NH_2(H_2O_2)(NH_3)_2 + Cl^-$	-28.3	-24.5	-24.5	-22.1	(3b⁗‴)
	$CH_3NH_2(NH_3) + Cl^-(H_2O_2) + NH_3$	-32.0	-31.7	-31.4	-42.1	(3b⁗⁗)
	$CH_3NH_2(H_2O_2) + Cl^-(NH_3)_2$	-32.4	-29.8	-29.8	-31.9	(3b⁗⁗′)
	$CH_3NH_2(NH_3)_2 + Cl^-(H_2O_2)$	-39.4	-37.0	-37.2	-38.3	(3b⁗⁗″)
	$CH_3NH_2+Cl^-(NH_3)_2(H_2O_2)$	-45.0	-42.1	-42.5	-41.6	(3b⁗⁗‴)

Table S4. Reaction energetics (kcal/mol) of $HOO^-(NH_3)(H_2O)$ + CH_3Cl S_N2 reactions in relative to the most stable reactants. Values are given by CCSD(T)/aug-cc-pVTZ//MP2/6-311++G(d,p) method.

Attacking Nucleophile	Products	ΔE	Δ(E+ZPE)	ΔH(298.15K)	ΔG(298.15K)	
HOO^- $(H_2O)(NH_3)$	$CH_3OOH+Cl^-+NH_3+H_2O$	-6.7	-8.5	-7.3	-21.6	(1_1a)
	$CH_3OOH+Cl^-(NH_3)+H_2O$	15.7	-16.6	-15.9	-24.5	(1_1a′)
	$CH_3OOH+Cl^-(H_2O)+NH_3$	-21.9	-22.4	-22.0	-30.6	(1_1a″)
	$CH_3OOH(H_2O)+Cl^-(NH_3)$	-23.2	-21.9	-21.7	-22.0	(1_1a‴)
	$CH_3OOH(NH_3)(H_2O)+Cl^-$	-25.0	-22.1	-21.9	-18.6	(1_1a⁗)
	$CH_3OOH+Cl^-(NH_3)(H_2O)$	-30.0	-29.3	-28.7	-32.1	(1_1a⁗′)
	$CH_3OOH(NH_3)+Cl^-(H_2O)$	-30.7	-29.2	-29.1	-29.6	(1_1a⁗″)
NH_2^- $(H_2O_2)(H_2O)$	$CH_3NH_2+H_2O+H_2O_2+Cl^-$	-1.4	-2.3	-1.4	-15.4	(1_1b)
	$CH_3NH_2+Cl^-(H_2O)+HOOH$	-16.7	-16.2	-16.2	-24.5	(1_1b′)
	$CH_3NH_2(H_2O)(H_2O_2)+Cl^-$	-22.1	-18.7	-18.6	-15.4	(1_1b″)
	$CH_3NH_2+Cl^-(H_2O_2)+H_2O$	-25.6	-25.9	-25.6	-33.3	(1_1b‴)
	$CH_3NH_2(H_2O_2)+Cl^-(H_2O)$	-28.6	-26.3	-26.4	-26.2	(1_1b⁗)
	$CH_3NH_2(H_2O)+Cl^-(H_2O_2)$	-34.8	-32.9	-32.9	-34.2	(1_1b⁗′)
	$CH_3NH_2+Cl^-(H_2O)(H_2O_2)$	-39.5	-37.3	-37.6	-36.7	(1_1b⁗″)
HO^- $(H_2O_2)(NH_3)$	$CH_3OH+NH_3+H_2O_2+Cl^-$	0.6	-0.2	0.7	-14.1	(1_1c)
	$CH_3OH+Cl^-(NH_3)+HOOH$	-8.5	-8.3	-8.0	-17.0	(1_1c′)
	$CH_3OH(H_2O_2)+Cl^-(NH_3)$	-16.6	-14.6	-14.4	-15.5	(1_1c″)
	$CH_3OH(NH_3)(H_2O_2)+Cl^-$	-18.3	-14.9	-14.6	-11.7	(1_1c‴)
	$CH_3OH+Cl^-(H_2O_2)+NH_3$	-23.7	-23.8	-23.5	-32.0	(1_1c⁗)
	$CH_3OH(NH_3)+Cl^-(H_2O_2)$	-30.6	-29.0	-28.8	-31.2	(1_1c⁗′)
	$CH_3OH+Cl^-(NH_3)(H_2O_2)$	-32.0	-30.5	-30.3	-30.5	(1_1c⁗″)

Table S5. Calculated energies (kcal/mol) of the stationary points relative to the reactants for the $HOO^-(NH_3)_n + CH_3Cl$ reactions given by CCSD(T)/aug-cc-pVTZ//MP2/6-311++G(d,p) method.

	ΔE	ΔE + ZPE	ΔH(298.15K)	ΔG(298.15K)
		n = 0		
$HOO^- + CH_3Cl$	0.0	0.0	0.0	0.0
0aRC-1	-16.3	-15.3	-15.3	-7.6
0aRC-2	-15.8	-14.9	-14.7	-7.4
0aTS	-13.9	-13.2	-13.5	-4.8
0aPC	-65.6	-62.6	-63.3	-53.5
$CH_3OOH + Cl^-$	-45.3	-42.9	-43.1	-40.4
		n = 1		
$HOO^-(NH_3) + CH_3Cl$	0.0	0.0	0.0	0.0
1aRC	-14.3	-13.1	-12.7	-5.0
1aTS	-10.2	-8.7	-8.9	0.5
1aPC-1	-60.2	-57.0	-57.0	-47.6
1aPC-2	-58.7	-55.6	-55.5	-47.5
$CH_3NH_2 + NH_3 + Cl^-$	-30.5	-29.4	-28.9	-35.1
		n = 2		
$HOO^-(NH_3)_2 + CH_3Cl$	0.0	0.0	0.0	0.0
2aRC-1	-13.0	-12.2	-11.7	-4.3
2aRC-2	-12.6	-11.9	-11.2	-3.7
2aRC-3	-12.3	-11.7	-10.9	-4.0
2aRC-4	-9.7	-9.0	-8.3	-0.2
2aTS-1	-7.2	-5.9	-6.0	4.2
2aTS-2	-4.5	-3.6	-3.5	6.2
2aPC-1	-56.2	-52.2	-52.8	-40.4
2aPC-2	-54.0	-51.0	-51.0	-41.5
$CH_3NH_2 + 2NH_3 + Cl^-$	-17.3	-18.2	-17.4	-31.7
		n = 3		
$HOO^-(NH_3)_3 + CH_3Cl$	0.0	0.0	0.0	0.0
3aRC-1	-13.0	-11.7	-11.5	-2.9
3aRC-2	-12.8	-11.9	-11.1	-4.1
3aTS-1	-6.4	-4.8	-5.1	4.4
3aTS-2	-5.2	-3.9	-3.8	5.4
3aPC-1	-53.0	-50.3	-50.0	-40.7
3aPC-2	-53.0	-49.1	-49.5	-38.7
3aPC-3	-53.0	-49.1	-49.5	-38.7
3aPC-4	-52.8	-48.9	-49.4	-38.5
$CH_3NH_2 + 3NH_3 + Cl^-$	-7.4	-10.2	-8.9	-33.4

Table S6. Calculated energies (kcal/mol) of the stationary points relative to the reactants for the $NH_2^-(HOOH)_{0,1}(NH_3)_{n-1}$ + CH_3Cl reactions given by CCSD(T)/aug-cc-pVTZ//MP2/6-311++G(d,p) method.

	ΔE	ΔE + ZPE	ΔH(298.15K)	ΔG(298.15K)
n = 0				
NH_2^- + CH_3Cl	0.0	0.0	0.0	0.0
0bRC-1	-14.6	-13.4	-13.6	-7.0
0bTS-1	-13.6	-12.5	-13.1	-5.0
0bPC-1	-80.3	-74.9	-75.8	-67.9
CH_3NH_2 + Cl^-	-68.5	-63.6	-64.2	-62.1
n = 1				
NH_2^-(HOOH)+CH_3Cl	0.0	0.0	0.0	0.0
1bRC-1	-11.6	-10.8	-10.4	-2.8
1bTS-1	-2.8	-2.0	-2.0	6.9
1bPC-1	-63.8	-59.1	-59.3	-49.9
CH_3NH_2 + HOOH + Cl^-	-27.9	-25.8	-25.3	-32.3
n = 2				
NH_2^-(HOOH)(NH_3) + CH_3Cl	0.0	0.0	0.0	0.0
2bRC-1	-19.8	-18.4	-17.6	-10.1
2bRC-2	-10.3	-9.5	-9.5	-0.2
2bTS-1	-2.9	-1.2	-1.9	9.9
2bTS-2	-2.1	-1.5	-2.1	10.0
1bPC-1	-65.0	-59.5	-60.1	-48.9
1bPC-2	-58.0	-53.0	-53.9	-42.1
CH_3NH_2 + HOOH + NH_3 + Cl^-	-18.8	-18.2	-17.6	-32.3
n = 3				
NH_2^-(HOOH)(NH_3)$_2$ + CH_3Cl	0.0	0.0	0.0	0.0
3bRC-1	-21.8	-20.2	-19.7	-11.4
3bTS-1	-2.1	-0.1	-1.1	12.8
3bPC-1	-66.2	-60.6	-61.4	-48.7
CH_3NH_2 + HOOH + 2NH_3 + Cl^-	-10.2	-11.2	-10.5	-33.8

Table S7. Overall barriers of HOO^--S_N2 and NH_2^--S_N2 pathway and their differences of $HOO^-(NH_3)_{n=0-3}$ + CH_3Cl.

n	$\triangle E^{\ddagger}_{HOO-}$	$\triangle E^{\ddagger}_{NH2-}$	$\boldsymbol{\Delta\Delta E^{\ddagger}}$	$\triangle H^{\ddagger}_{HOO-}$	$\triangle H^{\ddagger}_{NH2-}$	$\boldsymbol{\Delta\Delta H^{\ddagger}}$	$\triangle G^{\ddagger}_{HOO-}$	$\triangle G^{\ddagger}_{NH2-}$	$\boldsymbol{\Delta\Delta G^{\ddagger}}$
0	-13.9	-13.6	0.2	-13.5	-13.1	0.4	-4.8	-5.0	-0.2
1	-10.2	-0.1	10.0	-8.9	0.3	9.1	0.5	10.3	9.8
2	-7.2	3.8	11.0	-6.0	4.1	10.1	4.2	16.6	12.5
3	-6.4	5.9	12.3	-5.1	6.4	11.4	4.4	19.2	14.8

Note: $\Delta\Delta E^{\ddagger}_{ovr} = \triangle E^{\ddagger}_{ovr,\,NH2-} - \triangle E^{\ddagger}_{ovr,HOO-}$

Table S8. Internal barriers of HOO^--S_N2 and NH_2^--S_N2 pathway and their differences of $HOO^-(NH_3)_{n=0-3}$ + CH_3Cl.

n	$\triangle E^{\ddagger}_{int\ HOO-}$	$\triangle E^{\ddagger}_{int\ NH2-}$	$\boldsymbol{\Delta\Delta E^{\ddagger}_{int}}$	$\triangle H^{\ddagger}_{int\ HOO-}$	$\triangle H^{\ddagger}_{int\ NH2-}$	$\boldsymbol{\Delta\Delta H^{\ddagger}_{int}}$	$\triangle G^{\ddagger}_{int\ HOO-}$	$\triangle G^{\ddagger}_{int\ NH2-}$	$\boldsymbol{\Delta\Delta G^{\ddagger}_{int}}$
0	2.4	1.0	-1.4	1.8	0.5	-1.3	2.7	2.0	-0.7
1	4.1	8.8	4.7	3.9	8.4	4.5	5.5	9.8	4.3
2	5.8	16.9	11.1	2.3	15.7	13.4	4.4	20.1	15.7
3	6.6	19.7	13.1	6.1	18.6	12.5	7.3	24.1	16.8

Note: $\Delta\Delta E^{\ddagger}_{int} = \triangle E^{\ddagger}_{int,\,NH2-} - \triangle E^{\ddagger}_{int,HOO-}$

Table S9. Activation strain and energy decomposition analyses (kcal/mol) for the interaction between the anions and the solvent of the HOO^-(sol) (sol = NH_3, H_2O) and $NH_2^-(H_2O_2)(NH_3)_{n-1}$ complexes. (ADF[1], HF/TZ2P)

n		$\Delta E_{binding}$	ΔE_{def}	ΔE_{int}	ΔE_{Pauli}	$\Delta V_{elastic}$	ΔE_{oi}
1	$HOO^-(NH_3)$	-8.44	3.68	-12.12	40.88	-31.05	-21.95
2	$HOO^-(NH_3)_2$	-18.43	3.47	-21.91	51.42	-45.47	-27.86
3	$HOO^-(NH_3)_3$	-24.15	2.99	-27.14	51.35	-49.82	-28.67
1	$HOO^-(H_2O)$	-34.25	21.62	-55.87	50.88	-75.91	-30.84
2	$HOO^-(H_2O)_2$	-36.49	9.39	-45.88	74.27	-78.68	-41.47
3	$HOO^-(H_2O)_3$	-48.39	10.34	-58.73	90.28	-96.68	-52.33
1	$NH_2^-(H_2O_2)$	-36.57	19.16	-55.73	61.65	-82.36	-35.02
2	$NH_2^-(H_2O_2)(NH_3)$	-42.63	20.63	-63.26	69.58	-92.33	-40.50
3	$NH_2^-(H_2O_2)(NH_3)_2$	-47.08	22.01	-69.09	71.26	-97.95	-42.41

Fragmented method:

$HOO^-(NH_3)_n \rightarrow HOO^- + (NH_3)_n$

$HOO^-(H_2O)_n \rightarrow HOO^- + (H_2O)_n$

$NH_2^-(H_2O_2)(NH_3)_n \rightarrow NH_2^- + (H_2O_2)(NH_3)_n$

For $HOO^-(NH_3)_n$ and $NH_2^-(H_2O_2)(NH_3)_{n-1}$, the interaction between solvent molecules and the anion of the former is N-H···OOH^-, and the latter is N-H···NH_2^- and O-H···NH_2^-. The more polarized $Y^{\delta-}$-$H^{\delta+}$ bond in the $NH_2^-(H_2O_2)(NH_3)_{n-1}$ results in a favorable interaction.

Table S10. Energy (in eV) of the HOMO orbitals of the $HOO^{-}(NH_3)_n(H_2O)_m$ and $HO^{-}(NH_3)_n(H_2O)_m$ using MP2/6-311++G(d,p) method.

Nucleophile	HOMO Energy	Nucleophile	HOMO Energy	Nucleophile	HOMO Energy	Nucleophile	HOMO Energy
HOO^{-}	-3.1	NH_2^{-}	-1.3	HOO^{-}	-3.1	HO^{-}	-2.9
$HOO^{-}(NH_3)$	-3.9	$NH_2^{-}(HOOH)$	-3.5	$HOO^{-}(H_2O)$	-5.4	$HO^{-}(HOOH)$	-5.4
$HOO^{-}(NH_3)_2$	-4.6	$NH_2^{-}(HOOH)(NH_3)$	-4.0	$HOO^{-}(H_2O)_2$	-5.6	$HO^{-}(HOOH)(H_2O)$	-6.5
$HOO^{-}(NH_3)_3$	-4.8	$NH_2^{-}(HOOH)(NH_3)_2$	-4.4	$HOO^{-}(H_2O)_3$	-6.0	$HO^{-}(HOOH)(H_2O)_2$	-6.9
$HOO^{-}(NH_3)(H_2O)$	-5.2	$NH_2^{-}(HOOH)(H_2O)$	-4.6			$HO^{-}(HOOH)(NH_3)$	-6.1

Table S11 Selected bond distances (Å) of inv-S_N2-TS structures for $Y^-(NH_3)_n(H_2O)_m$ + CH_3Cl reactions as optimized by MP2/6-311++G(d,p) method.

inv-S_N2 transition structure	$r(X_{Nu}-C)^{‡}$	$r(C-Cl)^{‡}$	$\%(X_{Nu}-C)^{‡}$	$\%(C-Cl)^{‡}$	$\%L^{‡}$	$\%AS^{‡}$
$\mathbf{H_2N^-}\cdots CH_3\cdots Cl$	2.340	2.043	59.8	15.0	74.9	44.8
$\mathbf{HOO^-}\cdots CH_3\cdots Cl$	2.117	2.071	49.6	16.6	66.2	33.0
$\mathbf{HO^-}\cdots CH_3\cdots Cl$	2.158	2.090	51.8	17.7	69.4	34.1
$(H_3N)\mathbf{HOO^-}\cdots CH_3\cdots Cl$	2.067	2.104	46.1	18.5	64.5	27.6
$(H_3N)_2\mathbf{HOO^-}\cdots CH_3\cdots Cl$	2.034	2.130	43.7	19.9	63.7	23.8
$(H_3N)_3\mathbf{HOO^-}\cdots CH_3\cdots Cl$	2.028	2.139	43.3	20.4	63.8	22.9
$(HOOH)\mathbf{H_2N^-}\cdots CH_3\cdots Cl$	2.216	2.143	51.4	20.7	72.0	30.7
$(H_3N)(HOOH)\ \mathbf{H_2N^-}\cdots CH_3\cdots Cl$	2.246	2.120	53.4	19.4	72.8	34.0
$(H_3N)_2(HOOH)\mathbf{H_2N^-}\cdots CH_3\cdots Cl$	2.225	2.117	52.0	19.2	71.2	32.8
$(H_3N)(H_2O)\mathbf{HOO^-}\cdots CH_3\cdots Cl$	1.989	2.168	40.6	22.1	62.6	18.5
$(HOOH)(H_2O)\mathbf{H_2N^-}\cdots CH_3\cdots Cl$	2.207	2.137	50.8	20.3	71.1	30.4
$(HOOH)(H_3N)\mathbf{HO^-}\cdots CH_3\cdots Cl$	1.991	2.210	40.0	24.4	64.5	15.6

Note: The calculated O−C bond length in CH_3OOH is 1.412 Å, O−C bond length in CH_3OH is 1.422 Å, N−C bond length in CH_3NH_2 is 1.470 Å, C−Cl bond length in CH_3Cl is 1.760 Å.

Table S12 NPA charge distributions of inv-S_N2-TS structures for $X^-(NH_3)_n(H_2O)_m + CH_3Cl$ reactions.

inv-S_N2 transition structure	X_{Nu}	q(X_{Nu})	q(C)	q(Cl)	q(CH_3)	%$L^{\ddagger}$	Δq(Cl-O/N)
HO$^-\cdots CH_3\cdots Cl$	O	-1.221	-0.164	-0.538	0.381	69.4	0.683
H_2N $^-\cdots CH_3\cdots Cl$	N	-1.379	-0.239	-0.482	0.321	74.9	0.897
HOO$^-\cdots CH_3\cdots Cl$	O	-0.652	-0.177	-0.513	0.374	66.2	0.138
(H_3N)**HOO**$^-\cdots CH_3\cdots Cl$	O	-0.654	-0.154	-0.547	0.395	64.5	0.107
$(H_3N)_2$**HOO**$^-\cdots CH_3\cdots Cl$	O	-0.661	-0.134	-0.571	0.414	63.7	0.090
$(H_3N)_3$**HOO**$^-\cdots CH_3\cdots Cl$	O	-0.668	-0.133	-0.580	0.419	63.8	0.088
(HOOH)**H_2N**$^-\cdots CH_3\cdots Cl$	N	-1.315	-0.197	-0.567	0.357	72.0	0.748
(H_3N)(HOOH) **H_2N**$^-\cdots CH_3\cdots Cl$	N	-1.312	-0.206	-0.546	0.347	72.8	0.766
$(H_3N)_2$(HOOH)**H_2N**$^-\cdots CH_3\cdots Cl$	N	-1.312	-0.202	-0.547	0.357	71.2	0.765
$(H_3N)(H_2O)$**HOO**$^-\cdots CH_3\cdots Cl$	O	-0.635	-0.117	-0.606	0.432	62.6	0.029
(HOOH)(H_2O)**H_2N**$^-\cdots CH_3\cdots Cl$	N	-1.301	-0.196	-0.566	0.361	71.1	0.735
(HOOH)(H_3N)**HO**$^-\cdots CH_3\cdots Cl$	O	-1.171	-0.098	-0.645	0.442	64.5	0.526

Table S13. Formation energy (kcal/mol) of $HOO^-(sol)_n$ anions with sol as NH_3 and H_2O using CCSD(T)/aug-cc-pVTZ//MP2/6-311++G(d,p) level of theory.

n		[a]ΔE_f	ΔH_f	ΔG_f		ΔE_f	ΔH_f	ΔG_f	[c]$\Delta\Delta E_f$	$\Delta\Delta H_f$	$\Delta\Delta G_f$
0	HOO^-	0	0	0							
					Sol = H_2O						
1	[b]$HOO^-(H_2O)$	-27.1	-25.8	-16.5	$HO^-(H_2O_2)$	-27.1	-25.8	-16.5	0	0	0
2	$HOO^-(H_2O)_2$	-46.3	-43.5	-25.9	$HO^-(H_2O_2)(H_2O)$	-46.8	-43.7	-27.0	0.5	0.2	1.1
3	$HOO^-(H_2O)_3$	-64.1	-59.3	-30.4	$HO^-(H_2O_2)(H_2O)_2$	-65.1	-60.1	-32.1	1.0	0.8	1.7
					Sol = NH_3						
1	$HOO^-(NH_3)$	-14.8	-14.2	-5.4	$NH_2^-(H_2O_2)$	-12.1	-11.9	-2.1	-2.7	-2.3	-3.3
2	$HOO^-(NH_3)_2$	-28.0	-25.6	-8.7	$NH_2^-(H_2O_2)(NH_3)$	-21.2	-19.6	-2.1	-6.8	-6	-6.6
3	$HOO^-(NH_3)_3$	-37.9	-34.2	-7.0	$NH_2^-(H_2O_2)(NH_3)_2$	-29.9	-26.7	-0.6	-8	-7.5	-6.4
					Sol = $(NH_3)(H_2O)$						
	$HOO^-(NH_3)(H_2O)$	-37.2	-34.7	-18.3	$NH_2^-(H_2O_2)(H_2O)$	-29.6	-28.1	-10.3	-7.6	-6.6	-8
					$HO^-(H_2O_2)(NH_3)$	-38.6	-35.8	-18.9	1.4	1.1	0.6

Note:

[a]The ΔE_f is calculated as energy difference between the solvated species and the reactants HOO^- + n(sol)

[b]The optimized structure of $HOO^-(H_2O)$ is $HO^-(H_2O_2)$.

[c]$\Delta\Delta E_f = \Delta E_f(HOO^-) - \Delta E_f(HO^-)$ or $\Delta E_f(HOO^-) - \Delta E_f(NH_2^-)$

Table S14. The binding energy (kcal/mol) of $NH_2^-(H_2O_2)(NH_3)_{n-1}$ as calculated by energy difference between nucleophiles and corresponding solvent molecules. The CCSD(T)/aug-cc-pVTZ//MP2/6-311++G(d,p) level of theory was used.

		ΔE	***ΔH***	***ΔG***
n		$NH_2^- + nH_2O_2 + (n-1)NH_3 \rightarrow NH_2^-(H_2O_2)(NH_3)_{n-1}$		
1	$NH_2^-(H_2O_2)$	-40.5	-38.9	-29.9
2	$NH_2^-(H_2O_2)(NH_3)$	-49.7	-46.6	-29.9
3	$NH_2^-(H_2O_2)(NH_3)_2$	-58.3	-53.7	-28.4

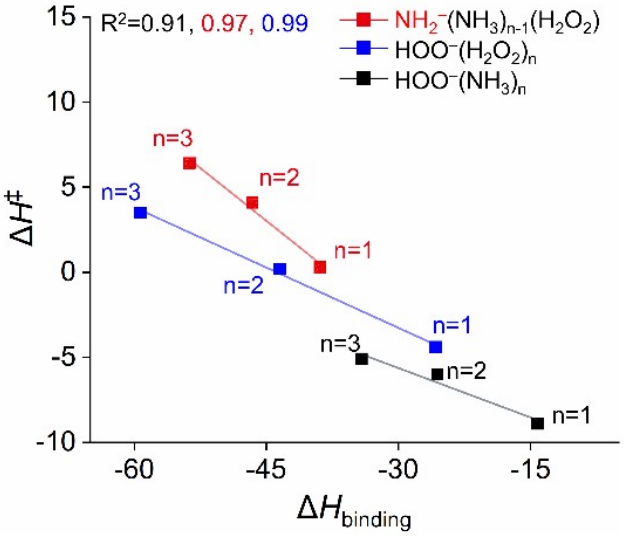

Table S15. Energies of inv-S_N2 transition states for $HOO^-(sol)_n$ + CH_3Cl reactions in relative to the most stable reactants.

n	Nu	ΔE‡	ΔH‡	ΔG‡	Nu	ΔE‡	ΔH‡	ΔG‡
			$HOO^-(H_2O)_n$ + CH_3Cl reaction					
0	HOO^-	-13.9	-13.4	-4.8	HO^-	-14.1	-14.0	-6.8
1	HOO^-	-5.2	-4.4	3.6	HO^-	-2.1	-1.0	7.8
2	HOO^-	-1.0	0.2	10.2	HO^-	1.8	2.9	14.2
3	HOO^-	2.4	3.5	13.5	HO^-	6.1	7.8	19.6
			$HOO^-(NH_3)_n$ + CH_3Cl reaction					
1	HOO^-	-10.8	-9.9	0.4	NH_2^-	-0.1	0.3	10.3
2	HOO^-	-7.8	-6.7	3.9	NH_2^-	3.8	4.1	16.6
3	HOO^-	-7.0	-5.9	5.7	NH_2^-	5.9	6.4	19.2
			$HOO^-(NH_3)(H_2O)$ + CH_3Cl reaction					
	HOO^-	-2.5	-1.6	7.3				
	NH_2^-	11.4	10.9	21.5				
	HO^-	2.2	3.3	13.1				

Reference

1 E.J. Baerends, T. Ziegler, J. Autschbach, D. Bashford, A. Bérces, F.M. Bickelhaupt, C. Bo, P.M. Boerrigter, L. Cavallo, D.P. Chong, L. Deng, R.M. Dickson, D.E. Ellis, M. van Faassen, L. Fan, T.H. Fischer, C. Fonseca Guerra, M. Franchini, A. Ghysels, A. Giammona, S.J.A. van Gisbergen, A.W. Götz, J.A. Groeneveld, O.V. Gritsenko, M. Grüning, S. Gusarov, F.E. Harris, P. van den Hoek, C.R. Jacob, H. Jacobsen, L. Jensen, J.W. Kaminski, G. van Kessel, F. Kootstra, A. Kovalenko, M.V. Krykunov, E. van Lenthe, D.A. McCormack, A. Michalak, M. Mitoraj, S.M. Morton, J. Neugebauer, V.P. Nicu, L. Noodleman, V.P. Osinga, S. Patchkovskii, M. Pavanello, P.H.T. Philipsen, D. Post, C.C. Pye, W. Ravenek, J.I. Rodríguez, P. Ros, P.R.T. Schipper, H. van Schoot, G. Schreckenbach, J.S. Seldenthuis, M. Seth, J.G. Snijders, M. Solà, M. Swart, D. Swerhone, G. te Velde, P. Vernooijs, L. Versluis, L. Visscher, O. Visser, F. Wang, T.A. Wesolowski, E.M. van Wezenbeek, G. Wiesenekker, S.K. Wolff, T.K. Woo, A.L. Yakovlev, **ADF2020**, SCM, Theoretical Chemistry, Vrije Universiteit, Amsterdam, The Netherlands, URL: http://www.scm.com.